Qatar Univ. Sci. J. (1999) 18 : 203 - 214

GRAVITY INVESTIGATION FOR DETECTING THE SUBSURFACE BASEMENT TOPOGRAPHY OF THE WESTERN PART OF BEHERA GOVERNORATE, NORTH EGYPT

By

Abou Shagar, S. and Mohammadin, M.

National Institute of Oceanography and Fisheries, Alexandria, Egypt

ملاحظات تثاقلية لتحديد طبوغرافية صخور القاعدة

للجزء الغربي من محافظة البحيرة - شمال مصر

السيدة أبو شجر محمود إسماعيل محمدون

المعهد القومي لعلوم البحار والمصائد - الأسكندرية - مصر

استخدمت تقنية التحليل الخطي من الدرجات الثانية ، الثالثة والرابعة ، وذلك لفصل كل من التأثيرين المحلي والنطاقي من شاذة البوجير ، وقد أعطت النتائج الخاصة بالدرجة الثانية أقرب النتائج واقعية مقارنة مع الأعمال المنشورة في هذا المجال .

وقد تم حساب نموذج ذو بعدين بإستخدام طريقة Talwani واتضح أن العمق يصل أقصاه في اتجاه الشرق والجنوب الشرقي حيث يتعدى حاجز ١٠ كم .

Key Words : Gravity - Basement - Topography - Behera - Egypt

ABSTRACT

One of the most effective tools for exploration of the subsurface basement topography is the gravity method. The Bouguer gravity map of the western part of Behera Governorate west of the Nile Delta of Egypt has been analyzed for this purpose. Trend analysis using linear, 2^{nd} , 3^{d}, and 4^{th} orders is used to separate the regional from local effects. The second order trend gave the optimum results when compared with the published works concerning the general subsurface structures in the Nile Delta and its surrounding area. Alternating NW-SE negative and positive anomalous trends are observed. 2-D models along two profiles are examined using the rapid method described by Talwani. Analysis of the obtained models show that the thickness of the sedimentary section increases towards the eastern and southeastern directions where it exceeds 10 km.

INTRODUCTION

The study area is located directly at the western side of the Nile Delta between Latitudes 30° 15' and 31° 10' N and Longitudes 30° 00' and 30° 40' E; covering an area of about 4500 km^2. The northern part of the study area includes five wells drilled during the seventieth, namely Mahmudiya, Kafr El-Dawar, Hosh Isa, South Damanhour, and North Dilingat. The geological history and tectonics of the Nile Delta and its adjacent western area have been studied by many authors:

Bayoumi and El-Gamili (1970) [1] studied the Bouguer gravity map of the northern part of the Western Desert and concluded that the dominating high gradient contour lines may be attributed to the crustal thickening. Abdel Dayem and Ali (1972) [2] studied the regional and local gravity effects at the area west of the Nile Delta. Zaghlul et al. (1979) [3] classified the sedimentary section of the Nile Delta and proposed a depth to the basement surface of about 10000 m. Awad (1975) [4] concluded that the type of the basement rocks may be of acidic or intermediate type as deduced from gravity investigation. Salim (1976) [5] considered that the Eocene/Oligocene and Early Miocene clastics represent deposits of an ancestral Nile which flowed in the NW direction into the Mediterranean Sea, and that an eastward shift of the Nile and its delta took place during Early to Middle Miocene. This situation may be due to crustal movements that affected northern Egypt.

According to [6] the Nile Delta began to form by the Eo-Nile and subsequently by a number of large rivers from Pliocene through Pleistocene to Recent times.

Following [7] a pronounced flexure (hinge line) affecting pre-Miocene formations extends nearly E-W across the mid-delta area, Fig.(1). Lower Tertiary and Upper Cretaceous formations show steep dip northward of this flexure zone. A system of normal faults prevails to the north of this hinge line.

The stratigraphy of the Nile Delta and its adjacent western part is summarized as follows (Fig. (2); [7]):

The Paleozoic is represented by Carboniferous and Permian overlying unconformably the basement. The Pre-Miocene formations include series from Upper Jurassic to Oligocene. They consist of typical close to shore shelf and lagoonal deposits. An overall regresssive shore line environment existsis for the Upper Mesozoic sequence, with significant unconformities at the top and bottom.

The Lower Cretaceous is represented by Neocomian/Barremian, Aptian and Albian with intercalations of clastics and limestone. The Upper Cretaceous is represented from Cenomanian to Senonian, consisting of limestone and dolomites.

The predominantly carbonate deposits of the Mesozoic and lowermost Tertiary are overlain by a huge section of Oligocene and Neogene clastics.

The depositional cycle from Lower to Upper Miocene is subdivided into three rock units, namely, the Sidi Salim Formation, the Qawasim Formation and the Rosetta Formation (from base to top). The Miocene cycle starts with a starved evaporitic sequence. The Sidi Salim Formation is formed of shale with interbedded dolomitic marls and rare sandstone. The Qawasim Formation is an irrigular sequence of thick sandstones and conglomerates. The Rosetta Formation is formed of anhydrite with interbedded thick claystone.

The Pliocene consists of the Abu Madi Formation, the Kafr El-Sheikh Formation and the El-Wastani Formation. The Abu Madi Formation is represented by thick bodies of sands with interbedded thin shales. The Kafr El-Sheikh Formation ranges in age from Lower to Middle Pliocene. It consists of interbedded, poorly consolidated sands with a clayey matrix. The El-Wastani Formation consists of quartoze sands with argillaceous interbeds.

The Holocene is represented by the Mit Ghamr and Bilqas formations. The Mit Ghamr Fomation consists of shelly sands, Coquina beds, clay and peat. Its age is the uppermost Pleistocene to Quaternary. The Bilqas Formation represents the top of the section and consists of sands, clays, plant remains and peat deposits.

Data Processing

The separation of regional from local gravity anomalies is a standard procedure in gravity interpretation. One of the most useful methods in doing this is the

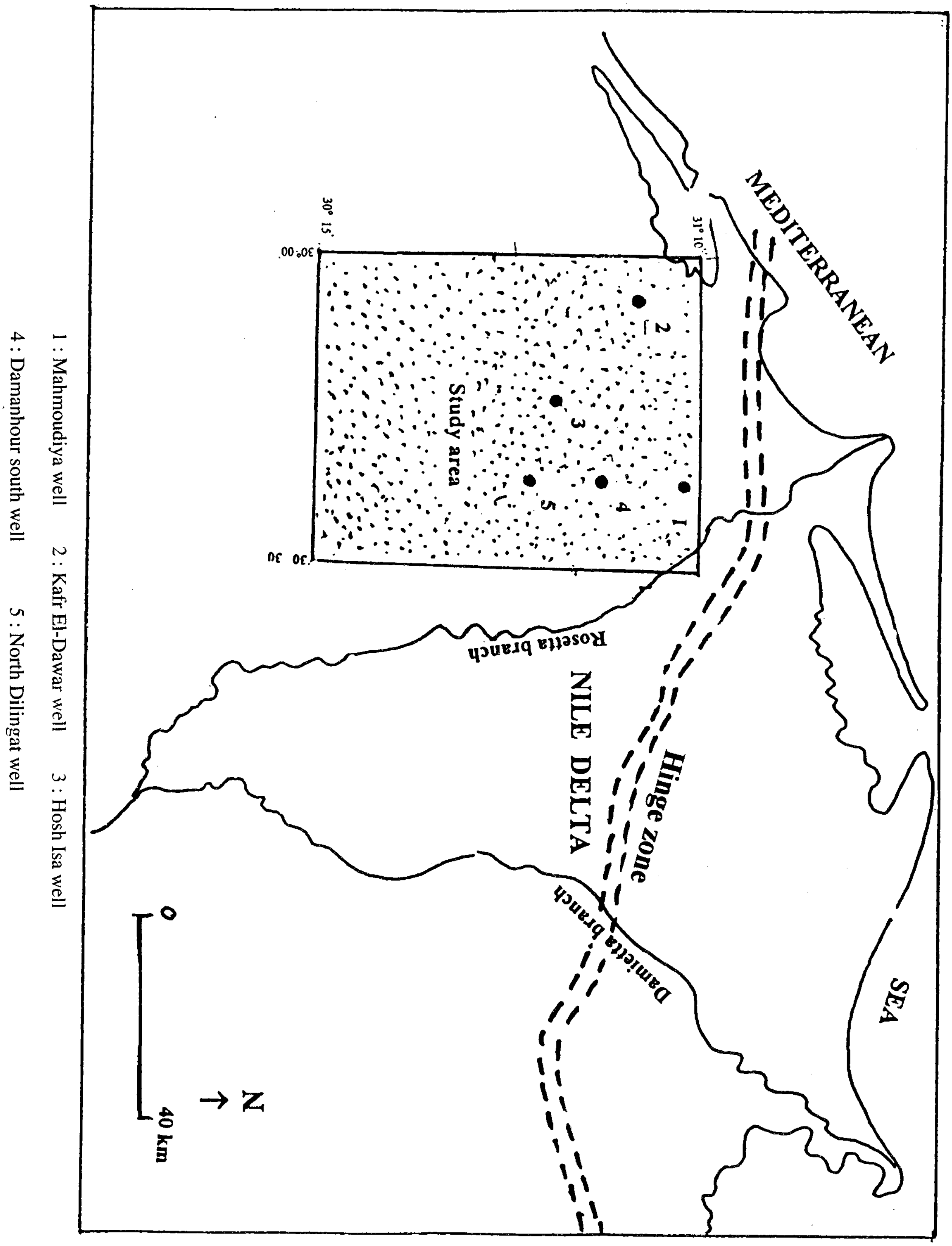

Figure (1): Location map of the study area with boreholes locations.

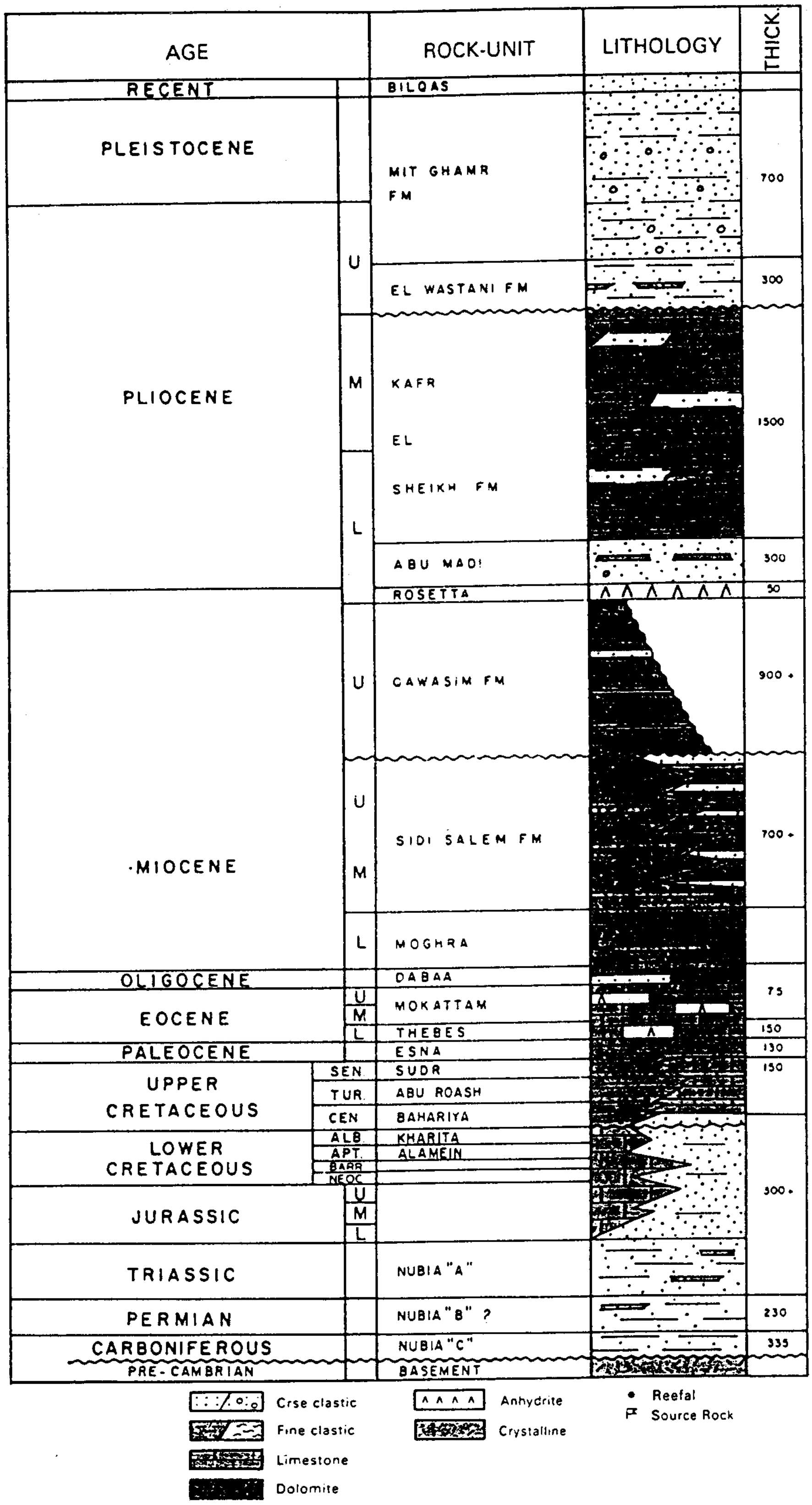

Figure (2): Generalized Stratigraphic column west of Nile Delta (after [7]) so-called statistical method. The theory of applying the statistical method can be explained as follows:

Local effects are considered as being random variables with a zero mean and variance ($\delta 2$) for all observations. Thus the residual component is regarded as being similar to the error found in any set of the observed data. The variable regional gravity can be expressed as a polynomial in two co-ordinates x,y as follows:

$$G_{reg.} = a_{00} + a_{01}y + a_{01}y^2 + \ldots\ldots . + a_{0h}y^h$$
$$+ a_{10}x + a_{11}xy + a_{12}xy^2 + \ldots\ldots\ldots$$
$$+ a_2x^2 + a_{21}x^2y + a_{22}x^2y^2 + Ö. + a_{r0}x^r + \ldots\ldots + a_{rh}x^ry^h \quad \ldots\ldots\ldots (1)$$

This polynomial can be written in terms of orthogonal polynomials:

$\xi'_0(x), \xi'_0(y), \xi'1(x), \xi'1(y), \ldots, \xi'r(x), \xi'n(y)$

and then

$$G_{reg.} = B00\, \xi'_0(x)\, \xi'_0(y) + B_{10}\, \xi'_1(x)\, \xi'_0(x) + \ldots$$
$$+ B_{rh}\, \xi'_r(x), \xi'_h(y) \ldots\ldots\ldots\ldots\ldots\ldots (2)$$

The coefficients can be determined using the equation

$$B = \sum_{q=0}^{r}\sum_{p=0}^{h} B_{qp}\, [\xi'^2_q(x)]\, S\, [\xi'^2_p(y)]$$
$$= S\, [\xi'^2_q(x)]\, S\, [\xi'^2_p(y)] = G_{qp} \quad \ldots\ldots\ldots\ldots (3)$$

where S denotes summation over all the observations, and

$$B_{qp} = G_{qp} / S\, [\xi'^2_q(x)]\, S[\xi'^2_p(y)] \quad \ldots\ldots\ldots\ldots (4)$$

Each observed value ($G_{ob.}$) has been assumed to differ from that of the corresponding regional value ($G_{reg.}$) by an error with zero mean and variance taking the same value for all the observations. It is assumed that the errors are uncorrelated. If in addition the errors are distributed normally then

$$Z_{qp} = G_{qp}/[S(_q{}^2(x))\, S(p^2(y))]^{1/2} \quad \ldots\ldots\ldots (5)$$

After obtaining the Greg. the local trend Gres. can be calculated by subtracting each regional value from the corresponding observed value

$$G_{res} = G_{ob.} - G_{reg.} \quad \ldots\ldots\ldots\ldots\ldots\ldots\ldots\ldots\ldots\ldots (6)$$

These calculations are carried out with data from a Bouguer gravity map covering the western part of Behera Governorate west of the Rosetta branch of the Nile Delta. The map has a scale of 1:250000 and is supplied by the Egyptian General Petroleum Corporation. The grid spacing of the data digitized from this map is 5 km.

DATA ANALYSIS AND INTERPRETATION

The underlying Bouguer anomaly map has a simple general trend, namely a gradual increase of the gravity values northward. The central part of the study area has a major distinctive negative anomaly trending NW-SE with gradual deccrease of gravity values towards the southern and southeastern directions (Fig.3). Contour line gradients are higher in the northern part of the study area than in its central and southwestern parts. Such a situation could reflect the presence of a major basin along the major negative anomaly which is surrounded by dense structures to the north, south and southwest.

To separate the regional from local effects three multiorder polynomials (second, third and fourth) were used. Three regional and three local gravity maps were prepared and are presented as Figs. 4 to 9.

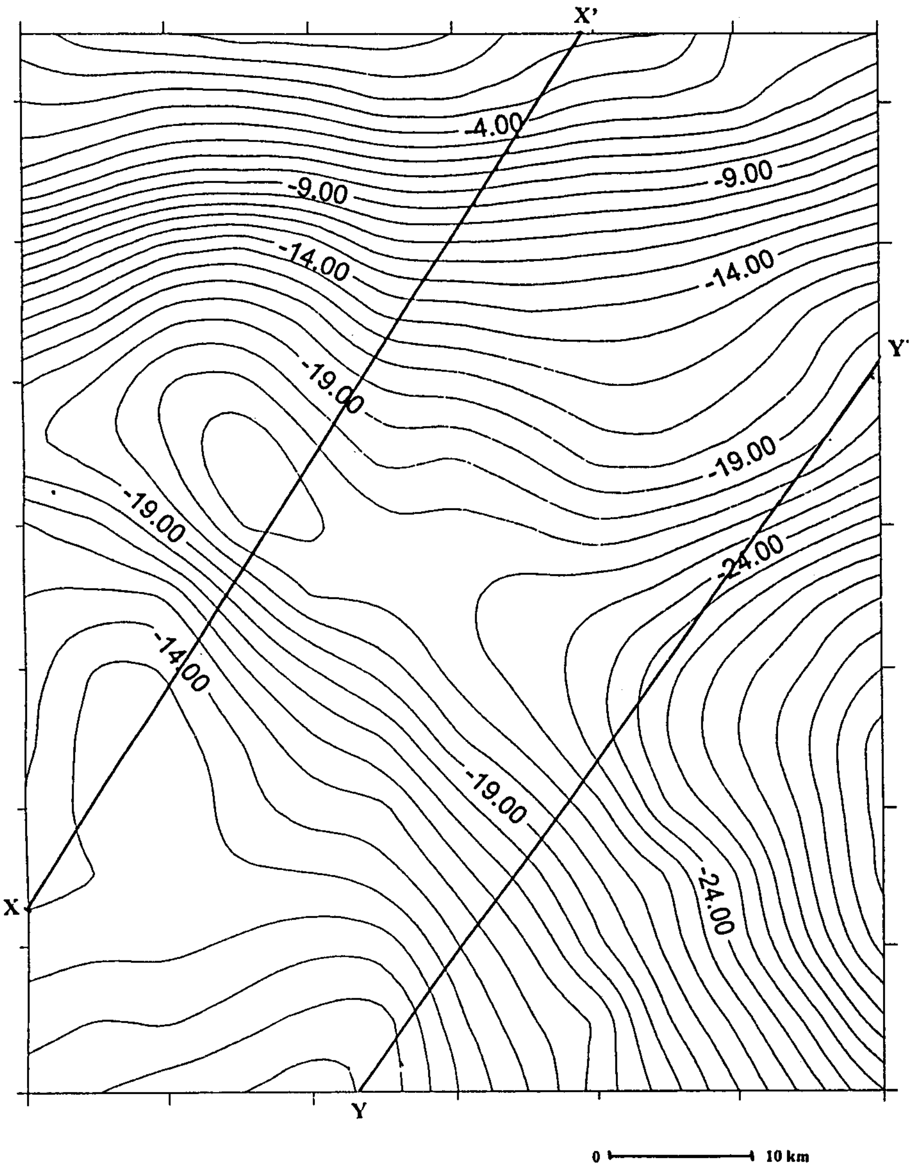

Figure (3): Bouguer Gravity map of the study area (C.I. 1 mgal)

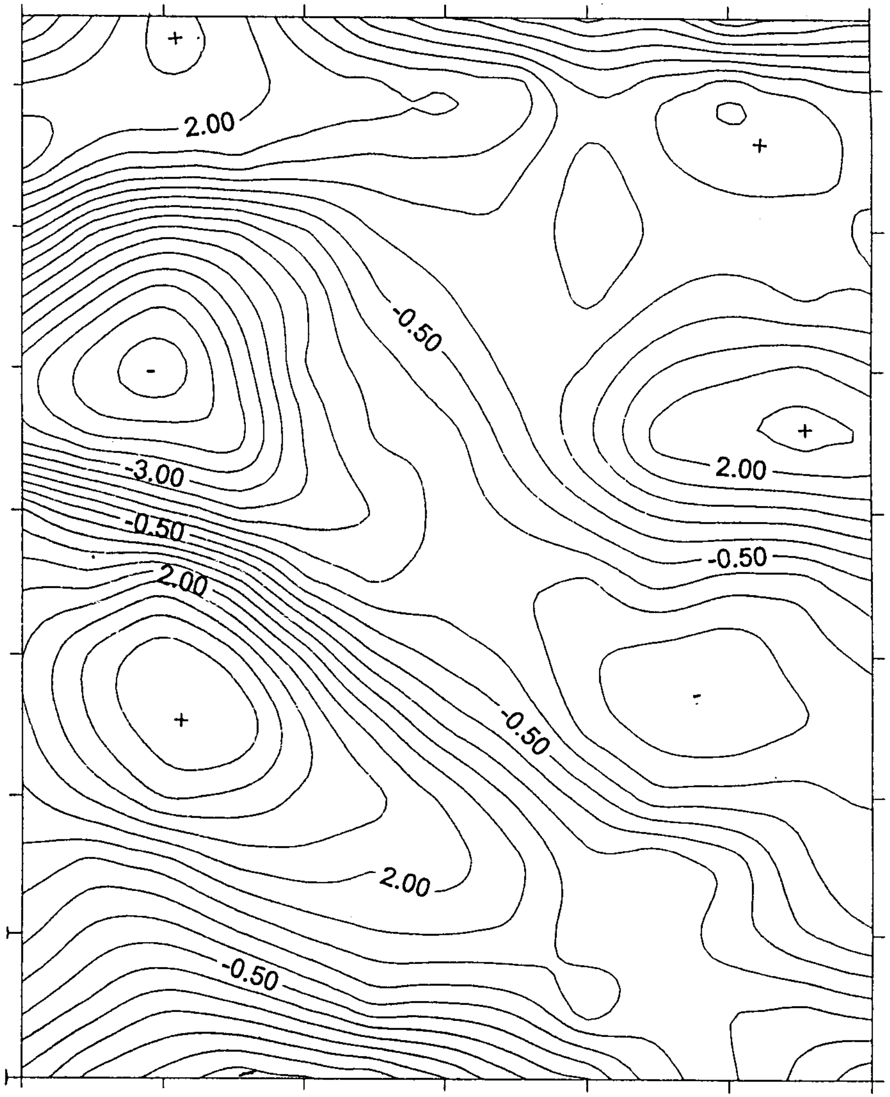

Figure (4) : Local Gravity map, second order (C.I. 0.5 mgal)

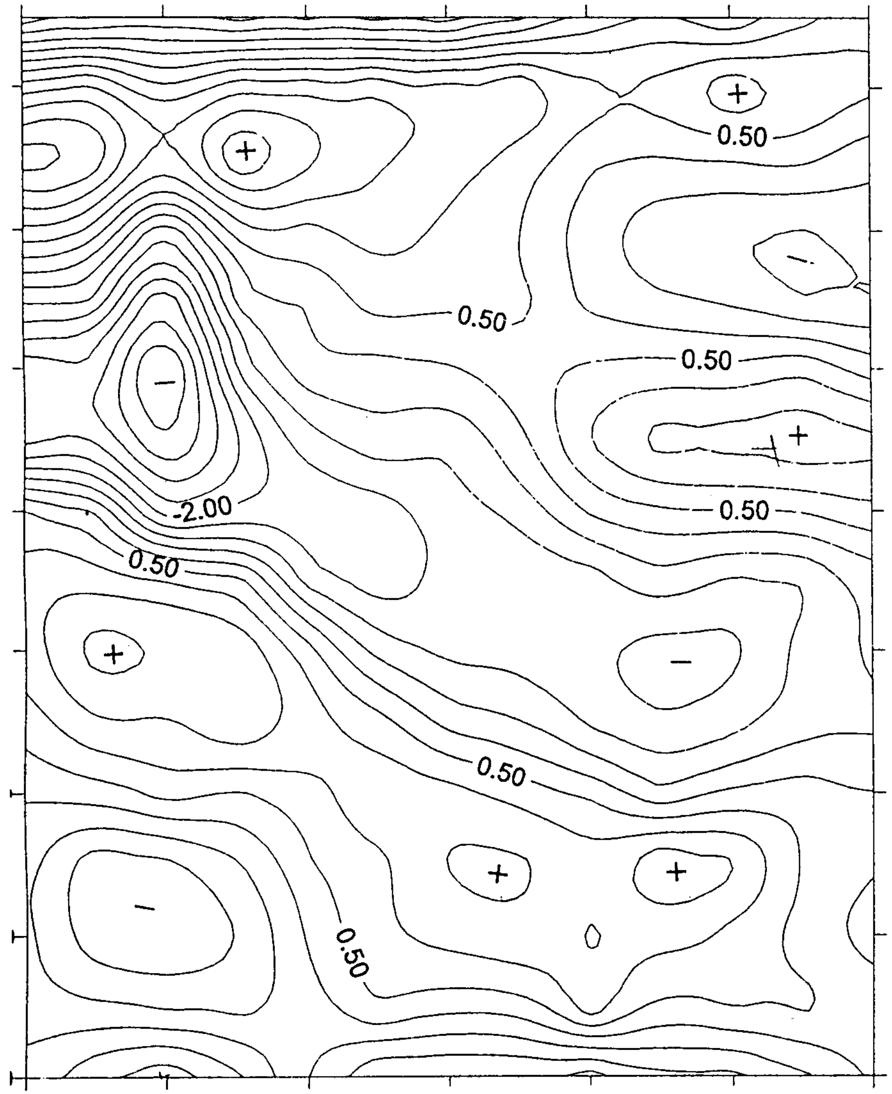

Figure (5) : Local Gravity map, third order (C.I. 0.5 mgal)

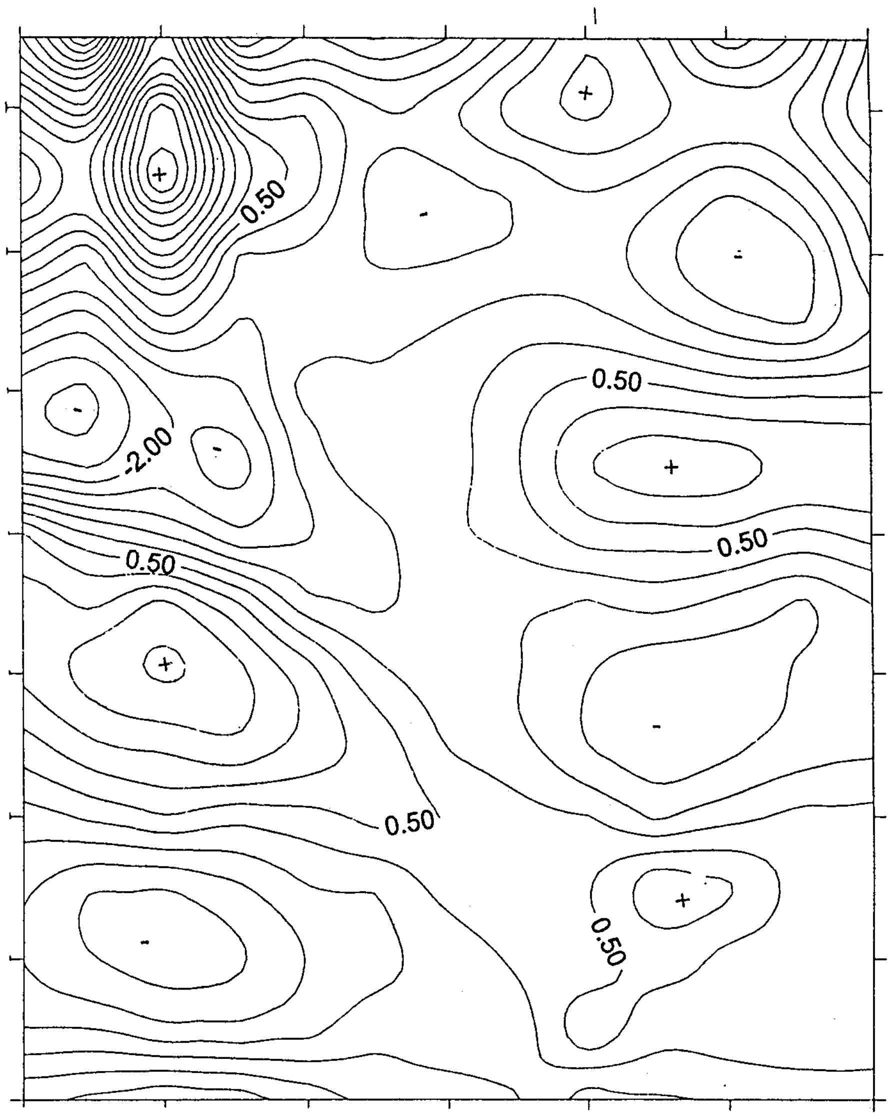

Figure (6) : Local Gravity map, fourth order (C.I. 0.5 mgal)

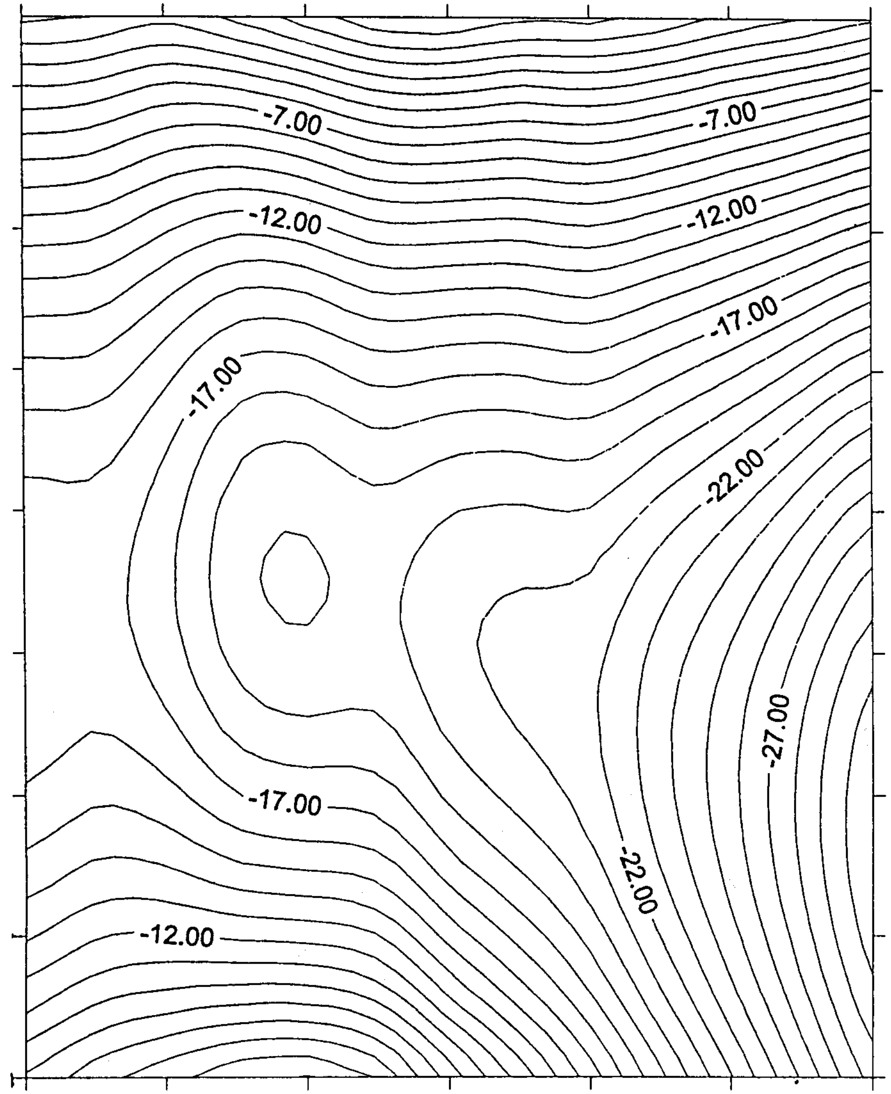

Figure (7): Regional Gravity map, second order (C.I. 1 mgal)

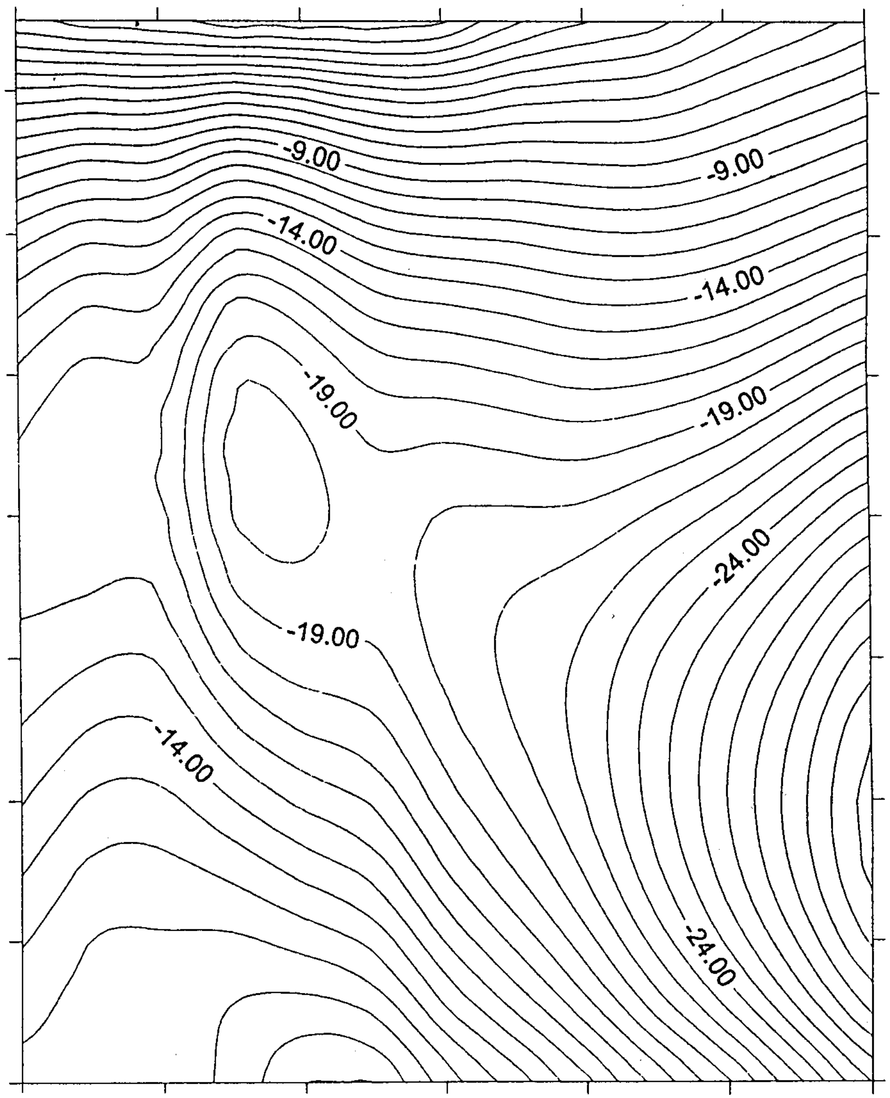

Figure (8): Regional Gravity map, third order (C.I. 1 mgal)

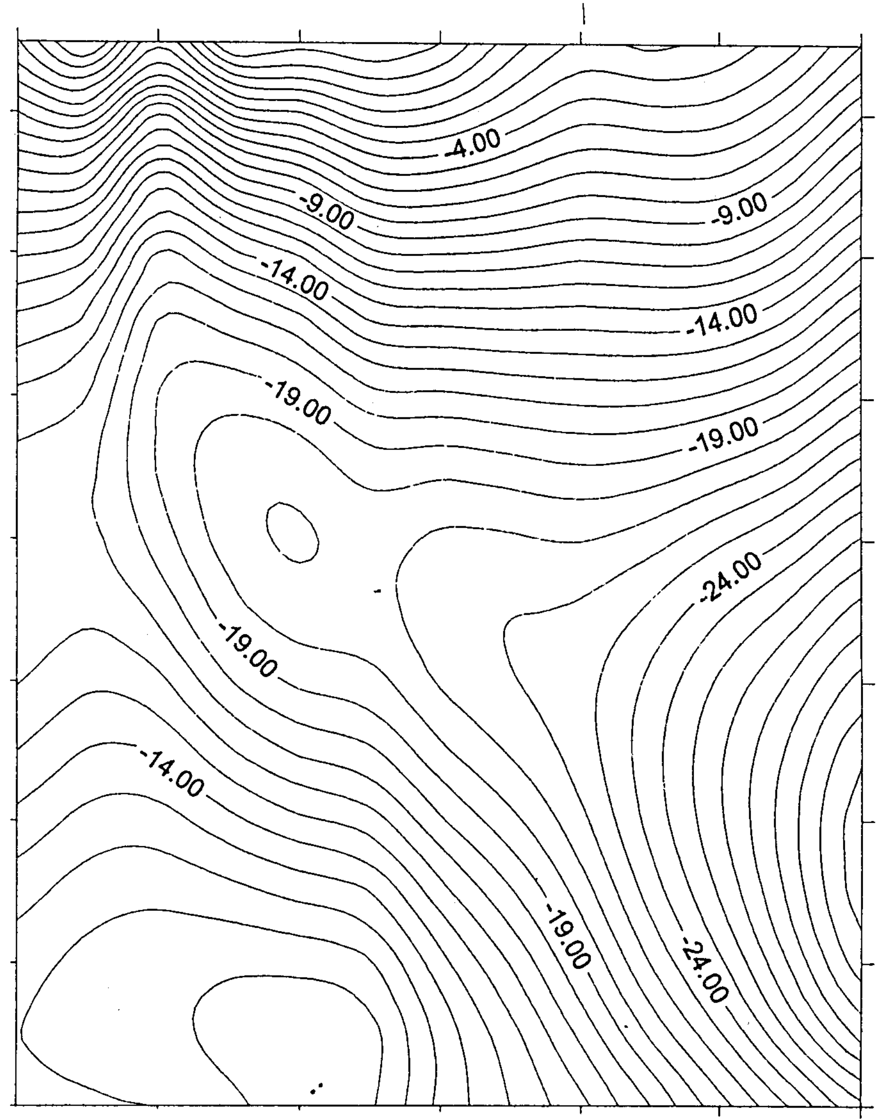

Figure (9): Regional Gravity map, fourth order (C.I. 1 mgal)

Comparison between the different local gravity maps of 2nd, 3d and 4th orders Figs . 4 to 6 , respectively, shows that the number of small anomalies increases with increasing the order of the polynomial degree. Alternating negative and positive anomalies trending W-E and NW-SE are noticed allover the local maps. A central NW-SE negative anomaly is noticed with different magnitude through the three orders. Comparison of the three regional gravity maps i.e. Figs.7 to 9 of the 2nd, 3d and 4th order, respectively, shows that the major structures represented by the main negative anomaly still exists. The second order map gives the optimum results [4, 5 and 7].

Quantitative interpretation has been carried out using the 2-D modeling technique of Talwani et al. [8]. Two profiles, XX' and YY',crossing the main anomalies (see Fig. 3) were used for calculating the gravity effect of subsurface geological structures, especially the basement topography. Before applying the algorithm the regional trend has been removed to deal only with the sedimentary cover down to as well the basement surface. The topography of the basement is included in the model, also additional information as given by [7]. Density values are extracted from some FDC logs of wells distributed allover the study area (see Fig. 1).

Figure (10) shows the calculated model (using the algorithm after [8]) along the XX' profile trending SW-NE and crossing the main Bouguer anomalies in the study area. The density of the basement is taken to be 2.7 g/cm^3 [5] and density values of the overlying sedimentary section are taken to range between 2.591 and 2.63 g/cm^3 as deduced from the FDC logs, with density contrast ranging between 0.07 to 0.109 gm/cm^3. The maximum depth to the basement surface is found to be 9.8 km, at the central part of the study profile, and the minimum depth is 6 km, at the extreme southwestern part of the study profile.

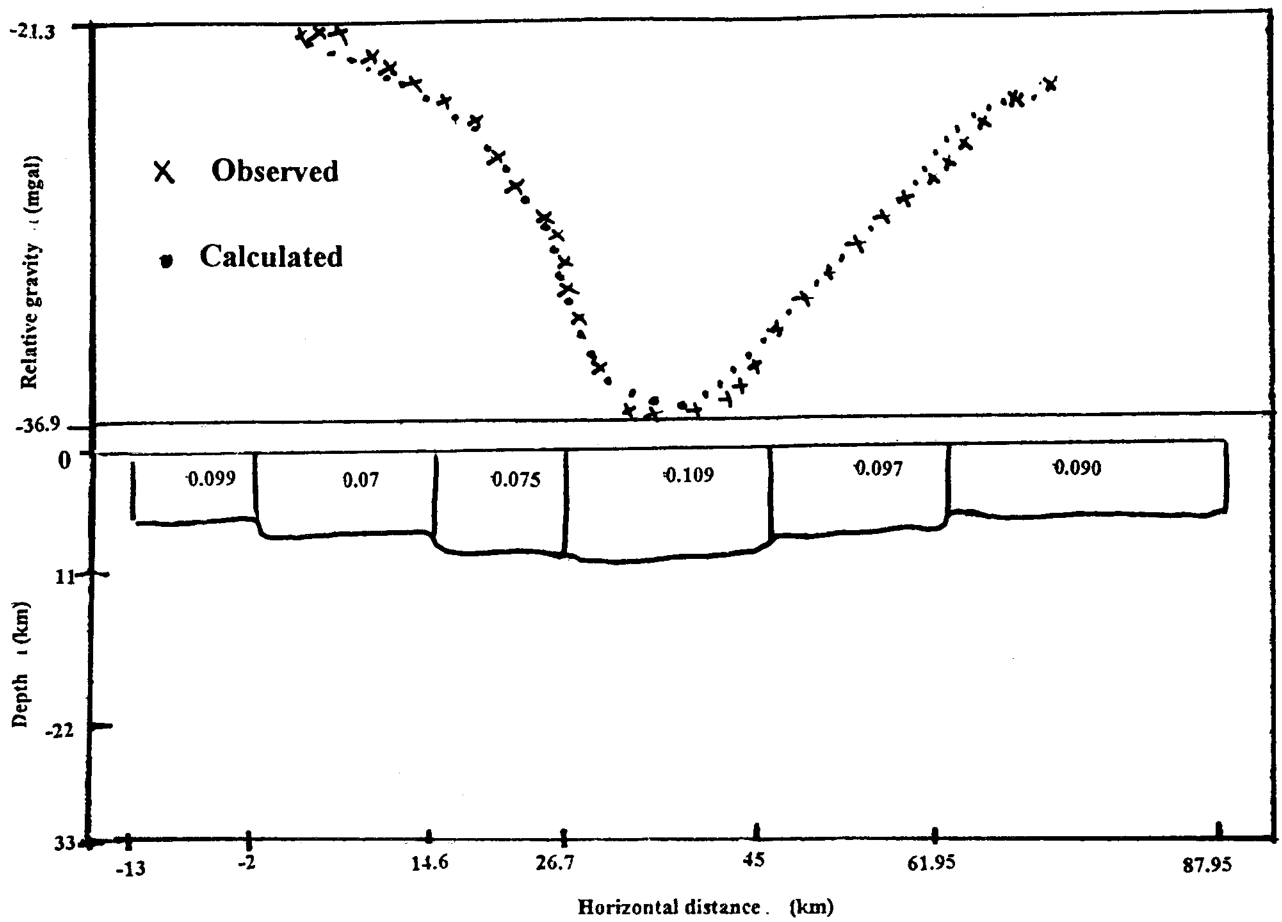

Figure (10) : 2-D Section along XX ' profile

Figure (11) shows the calculated model along the YY' profile trending at the same direction as the previous profile. Critical analysis of this profile shows nearly the same configuration as noticed for XX' on average density contrasts slightly lower than for the XX' profile. The basement density is taken as before (2.7 g/cm^3) while the density of the overlying sediments range between 2.605 and 2.619 g/cm^3 (as deduced from FDC logs) with contrasts ranging between 0.081 to 0.095 g/cm^3. The depths to the basement surface extend from 6.3 to 10.4 km.

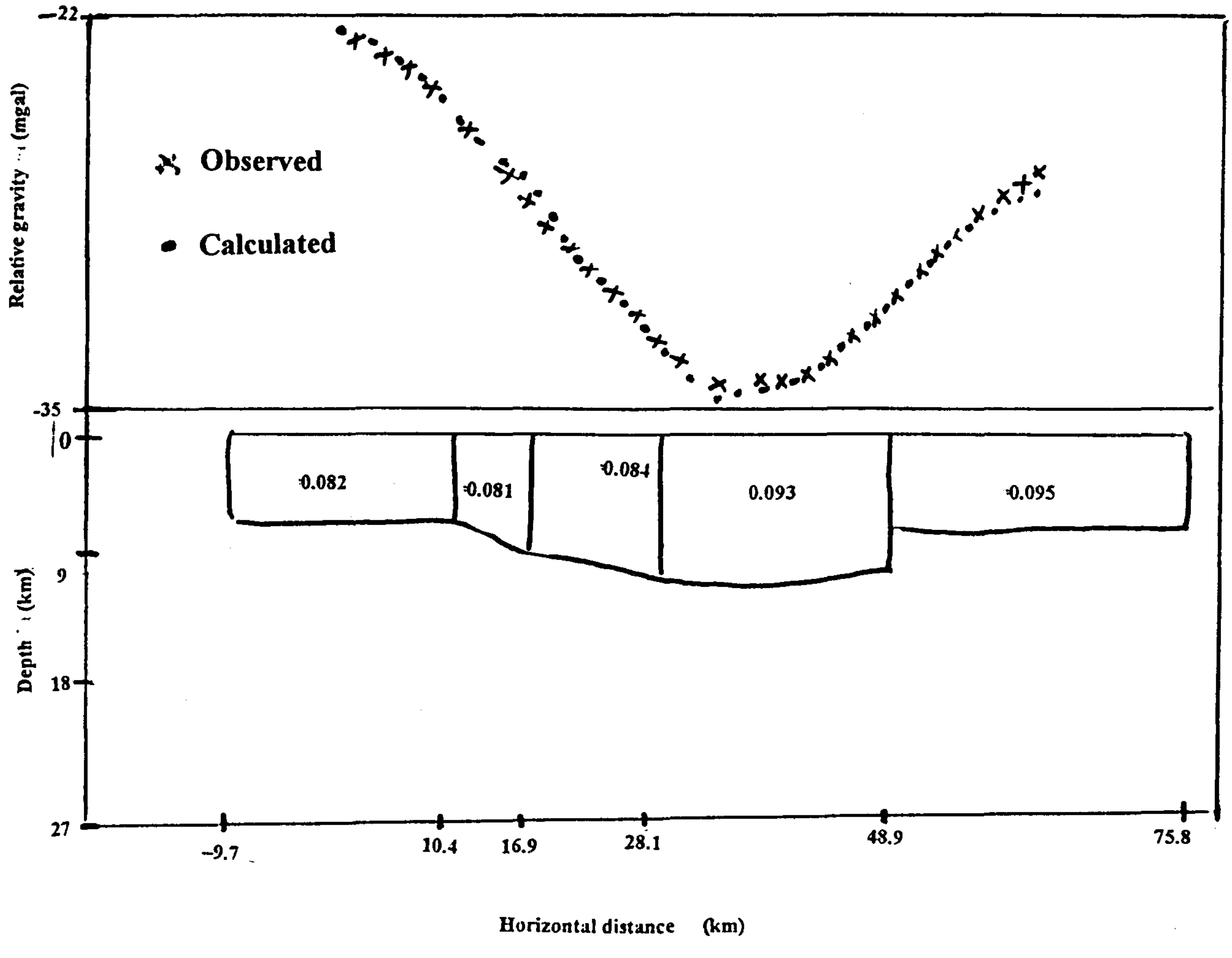

Figure (11): 2-D section along YY ' profile

CONCLUSIONS

This study revealed the following findings:

1) A major basin trending NW-SE dominates the central part of the study area.
2) The subsurface basement topography is clearly irregular. It ranges in depth from 6 to 10.4 km.
3) The basement depth increases as moving from western and southwestern parts of the study region towards the eastern and southeastern parts as well as towards the central part. This shows in turn that the basement depth tend to increase when moving towards the Nile Delta.

REFERENCES

1] Bayoumi, A. I. and El-Gamili, M. 1970: A geophysical study on the Fayum Rayan area with reference to its subsurface structure. 7th Arab Petroleum Cong., Paper No. 35, 15 p.

2] Abdel Dayem, M.M.and Ali, H.M. 1972: Two dimentional filtering of gravity fields in the Western Desert-Egypt, 8th Arab Petroleum Cong., Paper No. 44, 5p.

3] Zaghlul, Z. M., Andrawis, S.F. and Ayyad, S.N., 1979: New contribution to the stratigraphy of the Tertiary sediments of the Kafr El-Dawar well, northern Nile Delta, Egypt, Ann. Geol. Surv., Egypt (9), 292-307.

4] Awad, M.B., 1975: Investigation of geophysical anomalies of some localities of Northern part of Egypt for petroleum prospection. Ph.D. Thesis, Fac. Sci., Cairo Univ.

5] Salim, R., 1976: Evolution of Eocene/Miocene sedimentation patteren in parts of northern Egypt, AAPG Bull., 60: 34-64.

6] Said, R., 1983: Proposed classification of the Quaternary of Egypt, J.Afr. Earth Sci., 1: 41-45.

7] Schlumberger 1984: Well Evaluation Conference, Egypt. 244p.

8] Talwani, M., Worzel, J. and Landisman, M., 1959: Rapid gravity computation for two dimentional bodies with application to the Mendocina submarine fracture zone, J.Geophys.Res., 64:49-59.